



**HAL**  
open science

## The iron-responsive element (IRE)/iron-regulatory protein 1 (IRP1)-cytosolic aconitase iron-regulatory switch does not operate in plants

Nicolas Arnaud, Karl Ravet, Andrea Borlotti, Brigitte Touraine, Jossia Boucherez, Cécile Fizames, Jean-François Briat, Françoise Cellier, Frédéric Gaymard

### ► To cite this version:

Nicolas Arnaud, Karl Ravet, Andrea Borlotti, Brigitte Touraine, Jossia Boucherez, et al.. The iron-responsive element (IRE)/iron-regulatory protein 1 (IRP1)-cytosolic aconitase iron-regulatory switch does not operate in plants. *Biochemical Journal*, 2007, 405 (3), pp.523-531. 10.1042/BJ20061874 . hal-00478720

**HAL Id: hal-00478720**

**<https://hal.science/hal-00478720>**

Submitted on 30 Apr 2010

**HAL** is a multi-disciplinary open access archive for the deposit and dissemination of scientific research documents, whether they are published or not. The documents may come from teaching and research institutions in France or abroad, or from public or private research centers.

L'archive ouverte pluridisciplinaire **HAL**, est destinée au dépôt et à la diffusion de documents scientifiques de niveau recherche, publiés ou non, émanant des établissements d'enseignement et de recherche français ou étrangers, des laboratoires publics ou privés.

## The IRE/ IRP1-cytosolic aconitase iron regulatory switch does not operate in plants

Nicolas Arnaud<sup>1</sup>, Karl Ravet<sup>1</sup>, Andrea Borlotti<sup>2</sup>, Brigitte Touraine, Jossia Boucherez, Cécile Fizames, Jean-François Briat, Françoise Cellier and Frédéric Gaymard<sup>3</sup>

From the Laboratoire de Biochimie et Physiologie Moléculaire des Plantes UMR 5004 Agro-M/ CNRS/ INRA/ UMII, Bat 7, 2 place Viala, 34060 Montpellier cedex 1, France.

Short title: aconitase independent regulation of plant iron homeostasis

### Footnotes

Abbreviations used: ACO, aconitase; IRE, iron responsive element; IRP, iron regulatory protein; NO, Nitric Oxide; ROS, reactive oxygen species;

<sup>1</sup> these authors contributed equally to the work. <sup>2</sup> current address: Dipartimento di Produzione Vegetale, Università degli Studi di Milano, via Celoria, 2, 20133 Milano, Italy. <sup>3</sup> to whom correspondence should be addressed (E-mail: gaymard@supagro.inra.fr).

### Summary

Animal cytosolic aconitase and bacteria aconitase are able to switch to RNA binding proteins (IRPs), thereby playing a key role in the regulation of iron homeostasis. In the model plant *Arabidopsis*, we have identified three IRP1 homologues, named ACO1 to -3. To determine whether or not they may encode functional IRP proteins and regulate iron homeostasis in plants, we have isolated loss-of-function mutants in the three genes. The *aco1-1* and *aco3-1* mutants have a clear decrease in cytosolic aconitase activity. However, none of the mutants is affected in the accumulation of the ferritin transcript or protein in response to iron excess. *Cis*-acting elements potentially able to bind to the IRP have been searched *in silico* in the *Arabidopsis* genome. They appear to be very rare sequences, found in the 5'- or 3'-UTR of few genes unrelated to iron metabolism. They are therefore unlikely to play a functional role in the regulation of iron homeostasis. Taken together, our results demonstrate that, in plants, the cytosolic aconitase is not converted to IRP, and do not regulate iron homeostasis. In contrast to animals, the RNA binding

activity of plant aconitase, if any, would be more likely related to a structural element, rather than to a canonical sequence.

## Key words

cytosolic aconitase, iron, *Arabidopsis*, ferritin

## Introduction

As the major cofactor of proteins involved in essential processes like photosynthesis, respiration, DNA replication or nitrogen fixation, iron is an essential element for life. Nonetheless, in the free ionic form, iron is toxic as it can catalyze the formation of reactive oxygen species (ROS) through the Fenton reaction. These ROS damage the cell membranes, DNA and proteins [1, 2]. Thus, iron homeostasis has to be tightly regulated, to avoid starvation that impairs the metabolism, and to avoid excess that may lead to cell death. Iron homeostasis is strongly dependent on ferritins, which are iron-storage proteins, found in bacteria, animals and plants. Plant and animal ferritin structures are very similar, and are formed by 24 subunits arranged to form a hollow sphere able to sequester iron in a non-toxic and bioavailable form [3].

A major regulatory pathway of iron homeostasis in pluricellular eukaryotic organisms has been documented from studies with animal systems [3, 4]. In these systems, the balance between iron uptake and iron storage is mainly achieved by the post-transcriptional regulation of ferritin and transferrin receptor synthesis by the IRE/ IRP1-cytosolic aconitase iron switch. In the 5'-untranslated region of ferritin mRNA and in the 3'-untranslated region of transferrin receptor transcript are located specific sequences, named IREs (Iron-Responsive-Elements [5]). The IREs function as binding sites for two related *trans*-acting factors, namely the iron regulatory proteins IRP1 and IRP2. When bound to the IRE of the ferritin mRNA, the IRP inhibits translation of the transcript [4]. Conversely, the binding of IRP to the IREs found in the 3'-untranslated sequence of the transferrin receptor mRNA stabilizes the transcript, thus leading to the synthesis of the protein.

IRP1 is a bifunctional protein that, when iron is abundant, possesses a 4Fe-4S cluster and acts as a cytosolic aconitase. When iron level is low, the 4Fe-4S cluster disassembles and the apoprotein acquires IRP activity, thus repressing ferritin translation. High levels of iron lead to the 4Fe-4S cluster reconstitution and therefore to the protein aconitase activity. Exposure to nitric oxide (NO<sup>•</sup>) and ROS was shown to convert the aconitase into an IRP by releasing the cluster, consequently leading to the IRE binding, and finally modulating the expression of ferritins [6, 7]. IRP2 is an IRP1 homologue which does not contain a Fe-S cluster and thus has no aconitase activity. Its activity is primarily regulated by iron-dependent degradation [8].

Several reports suggested that the IRE/ IRP1-cytosolic aconitase could also operate in plants [9-11], making it a universal regulatory pathway in eukaryotic pluricellular organisms. Indeed, several lines of evidence suggest a putative relation between ferritins and aconitase activity. NO and oxidative stress have been shown to modulate the expression of ferritins in plants [11-13], and to inactivate the aconitase [10, 14], and thus potentially converting it into an IRP. However, indirect evidences are not in favor of an IRE/ IRP1-cytosolic aconitase regulatory switch in plants. Indeed, the synthesis of plant ferritins and iron transporters has been shown to be regulated at the transcriptional level in response to the iron status, and not at the mRNA stability or translational levels as described above for animal cells [12, 15]. IRE sequences are not found in the plant ferritin genes. No IRP activity is detectable in plant cell extracts by RNA shift experiments using animal IRE as a probe [16], or in a translational assay using animal ferritin mRNA and wheat germ extract [17]. However, it must be pointed out that the bacterial aconitase does have a RNA binding activity, but does not recognize a canonical IRE sequence [18, 19]. The potential RNA binding activity of plant aconitase was recently enforced by showing that an *Arabidopsis* aconitase protein is able to bind to the 5'-UTR of the superoxide dismutase *CDS2* gene [20].

In order to directly address the involvement of a putative IRP1-cytosolic aconitase regulatory switch in the regulation of ferritin expression in plants, we searched for IRP homologues in the *Arabidopsis* genome, identified three genes encoding putative aconitase, and isolated the corresponding loss-of function mutants. In the three mutants, the expression of genes involved in iron homeostasis was not altered, demonstrating that cytosolic aconitase, in contrast to animals and bacteria, are not involved in the regulation of iron metabolism in plants.

## EXPERIMENTAL

### Isolation of *aco* knock-out mutants

Mutants in the three aconitase genes *ACO1* (At4g35830), *ACO2* (At4g26970), *ACO3* (At2g05710) were identified in the collections from the Salk Institute [21] for *ACO2* (line Salk-054196), and *ACO3* (line Salk-013368) and from the GABI-Kat [22] for *ACO1* (line 138A08). Plants were back-crossed and homozygous mutant plants were identified by PCR on genomic DNA. The two T-DNA / gene junctions were amplified and sequenced to determinate the location of the T-DNA insertion.

### Plant Culture

Plants were grown on soil (Humin substrate N2 Neuhaus, Klasmann-Deilmann, Geeste, Germany) in a greenhouse at 23°C with a light intensity maintained above 300  $\mu\text{E}\cdot\text{s}^{-1}$  per  $\text{m}^2$  and a day/night regime of 16 h/ 8 h. For determining the expression pattern of *ACO* genes, wild type (Col ecotype) plants were grown in hydroponic conditions for 5 weeks as described [23]. The other studies were performed on 10 days old plantlets grown in liquid medium in sterile conditions [13]. For the iron-starvation treatment, plants were transferred in the same medium, except that Fe(III)-EDTA was omitted. For iron excess treatment, a mix of  $\text{FeSO}_4/ \text{Na}_3\text{-citrate}$  was added (final concentration in the medium: 300  $\mu\text{M}$   $\text{FeSO}_4/$  600  $\mu\text{M}$   $\text{Na}_3\text{-citrate}$ ).

### RNA preparation and analysis

Total RNA were extracted, and northern blot experiments were performed as indicated in Lobréaux et al. [24]. The *EF1 $\alpha$* , *AtFer1* and *IRT1* specific probes were obtained as described [13, 25]. The *AtFer3* specific probe consists in a chimeric fragment containing the 5'- and 3'- UTR regions of the *AtFer3* cDNA. The 5'-UTR region was amplified with thermostable *Pfu* DNA polymerase (Promega, Madison, USA) using the primers 5'-GGTACCTATATTCCCTCCTCCGCCACCACCAATC -3' and 5'-GAATTCAAACCGGAGACGAAATGGAGG -3' introducing a *Kpn* I and an *Eco*R I sites at the 5' and 3' end of the amplified fragment respectively. The 3'-UTR region was amplified using the primers 5'- TGGGAATTCTGCTTAATCTGAG -3' and 5'- GGGTACTAGTAAATATCAGTG -3' introducing an *Eco*R I and a *Spe* I sites at the 5' and 3' ends of the amplified fragment respectively. The fragment was cloned at the corresponding sites in pBluescript and sequenced. The specific probe (462 bp) was obtained by digesting the resulting construct by *Kpn* I and *Spe* I. The aconitase specific probes were amplified by PCR on genomic DNA as described above for *AtFer3*, cloned in pBluescript at the *Eco* RV site, and sequenced. The *ACO1* probe, located in the 3'-UTR, was amplified with the primers 5'-GAGTTGGCTTATTTTCGATCAGG-3' and 5'-GACTCGACAGTGATAATGTTTCC-3'. The two other *ACO* probes, located in the 5'-UTR, were amplified with 5'-CTTGACGAAATCTCTTCTCCGTCTC-3' and 5'-GAGCAAACCTCGAAAGGAGCGGAGAGCC-3' for *ACO2*, and 5'-CGCAGCCCTAGGCATTTTCG-3' and 5'-GGGGAAATGGTACCAAAGATCTACG-3' for *ACO3*. 25S RNA and specific probes were labeled, and hybridization were performed as described [13].

### Preparation of cytosolic and mitochondrial matrix extracts

All procedures were carried out at 4°C. Plantlets (50 g) were cut with a razor blade and ground in a mortar containing extraction buffer (330 mM sorbitol, 30 mM MOPS-BTP, 2 mM PMSF, 2 mM 2  $\beta$ -mercaptoethanol, 2 mM  $\text{Na}_3\text{-citrate}$ , 2 mM ascorbic acid, 1 mM EDTA, 10  $\mu\text{g}\cdot\text{ml}^{-1}$  leupeptin, 1%

PVP, pH 7.5) in ratio 1/3 w/v. The homogenate was filtered through two layers of Miracloth (Calbiochem, Merck Biosciences, Darmstadt, Germany), and centrifuged at 280 g for 10 min to remove the cell debris and the chloroplasts. The supernatant was centrifuged at 10800 g for 30 min. The resulting pellet contained mitochondria, while the supernatant corresponded to the cytosol and the membranes fractions. This supernatant was centrifuged at 100000 g for 45 min to pellet the membranes. Glycerol (final concentration 10%) was added to the resulting supernatant (cytosolic fraction), and samples were stored in liquid nitrogen until use. The pellet containing mitochondria was resuspended in 2 ml of lysis buffer (10 mM Tris-HCl, 2 mM 2  $\beta$ -mercaptoethanol, 2 mM Na<sub>3</sub>-citrate, 1 mM PMSF, 1 mM EDTA, 10  $\mu$ g.ml<sup>-1</sup> leupeptin, pH 7.2). Mitochondria were broken by vortexing and freezing three times the samples in liquid nitrogen. After a centrifugation at 100000 g for 45 min, the supernatant containing matrix proteins was recovered. Glycerol (final concentration 10%) was added, and samples were stored in liquid nitrogen. Protein concentration was determined according to Schaffner and Weissmann [26] using BSA as standard.

### **Enzymatic activities**

Aconitase activity was assayed at 20 °C in 100 mM Tris-HCl, 50 mM DL-isocitric acid (trisodium salt), pH 7.4, by measuring the production of *cis*-aconitate. The extinction coefficient used for *cis*-aconitate was of 3.6 mM<sup>-1</sup>. cm<sup>-1</sup> at 240 nm. The reaction was started by adding from 75  $\mu$ g to 150  $\mu$ g of protein in 1 ml final volume. Before measuring the citrate synthase activity, mitochondrial and cytosolic extracts were purified in a BioSpin 6 column (Bio-Rad, Hercules, USA) following the manufacturer's instructions to discard 2  $\beta$ -mercaptoethanol that negatively influences the activity. Citrate synthase activity was determined in 100 mM Tris-HCl, 0.1 mM 5,5'-dithiobis(2-nitrobenzoic acid) (DTNB), 0.2 mM acetyl-CoA, pH 8.0, from 50  $\mu$ g of protein extract in 1 ml final volume. After 5 min of incubation at 30°C, the reaction was initiated by adding oxaloacetic acid (1 mM final concentration) at room temperature. The reduction of DTNB was measured by detection of 2-nitro-5-thiobenzoic acid reduced form (TNB-SH). The extinction coefficient used for TNB-SH was of 13,8 mM<sup>-1</sup>. cm<sup>-1</sup> at 412 nm.

### **Immunodetection of ferritins**

Total protein extracts were prepared from 1 g of each sample as described [27]. Proteins were subjected to electrophoresis on a 13% polyacrylamide / 0.1% SDS gel according to Laemmli [28]. After electroblotting onto Hybond-P membrane (Amersham Biosciences), immunodetection of ferritin was performed using a rabbit polyclonal antiserum raised against purified AtFer1 protein [29] and the Aurora Western blotting kit (MP Biomedicals, Irvine, USA) following the manufacturer's recommendations.

### **Bioinformatics**

IRE motif searches were performed on *Arabidopsis thaliana* 5'- and 3'-UTR sequences (available at the TAIR website <http://www.arabidopsis.org/>) using a Perl script specially written for this purpose, and using the sequence CXXXXXCAGUGNYYYYY as consensus of the IRE loop. The constraints imposed in the script were as follow: N designs any of the 4 bases. The five bases noted X and Y are involved in the stem formation, and must be complementary (A/U, C/G) or form a stable weak interaction (U/G). For the putative bacterial *acn* binding site, the two paired motifs, ACACAAUGC and CAUUUU, as defined by Tang and Guest [18] were searched. To determine the probability for the motifs to occur by chance in the sequences, the SMILE software was used [30]. This algorithm allows dealing with structured motifs eventually associated by some distance constraints.

## RESULTS

### Identification of IRP-like proteins in *Arabidopsis*

In order to determine whether the animal IRE/ IRP regulatory system may have a counterpart in plants, we first try to identify IRP1 and IRP2 homologues in *Arabidopsis* genome. We identified three genes encoding aconitase hydratase, named *ACO1* (At4g35830), *ACO2* (At4g26970) and *ACO3* (At2g05710). *ACO1* corresponds to the gene previously identified by Peyret et al. [9]. The two others are identical to the genes recently identified by Moeder et al. [20]. The three proteins are closely related, and share more than 90% similarity, and have about 80% of similarity with IRP1 and IRP2 (Figure 1). The three cysteine residues (indicated by squares on Figure 1) in the IRP1 sequence, involved in the Fe-S cluster formation, are completely conserved in the three plant ACO proteins, suggesting that they could associate a cluster, and could have an aconitase activity. The crystal structure of the IRP1:ferritin H IRE complex allowed to identify amino acids directly interacting with the RNA loop ([31]; indicated by stars on Figure 1). Interestingly, most of these residues are conserved in the three plant ACO proteins (Figure 1), raising the hypothesis that plant ACO could bind IRE sequences.

### Isolation of *aco* loss-of-function mutants

To investigate the involvement of *Arabidopsis* aconitase genes in ferritin regulation, we have isolated knock-out mutants in the three corresponding genes from the Salk Institute [21] (for *ACO2*: line Salk054196, and for *ACO3*: line Salk013368) and the GABI-Kat [22] (for *ACO1*: line 138A08) collections. In the mutants, the two T-DNA flanking sequences were determined. The three mutants were named *aco1-1*, *aco2-1* and *aco3-1*. In the three mutant lines, the T-DNA were found to be

inserted in inverted tandem (Figure 2A). In *aco1-1*, the insertion is located in the 14th exon of the gene, and led to a small deletion of 5 bp, and to the insertion of 12 and 8 bp extra sequences at the 5'- and 3'-junctions respectively. In *aco2-1*, the insertion is located in the 6th exon, and led to a 413 bp deletion, and to the insertion of 12 bp extra sequence at the 3'-junction. In *aco3-1* mutant, the insertion was found to be located in the 5th exon, and led to a deletion of 8 bp, and to the addition of 5 bp extra sequence at the 3'-junction. The *aco3-1* line has been previously described by Moeder *et al.* and was named KO-661 [20]. Lines homozygous for the disruption were isolated, and used for further studies. When the mutants were grown in greenhouse, or in hydroponic cultures under controlled conditions, they displayed no macroscopic phenotype. Furthermore, changes in environmental parameters, such as light intensity or iron concentration in the culture solution, did not lead to any obvious phenotype (data not shown).

The expression of the three *ACO* genes was investigated in the *aco* mutant backgrounds by northern blot with specific probes corresponding to the three genes (Figure 2B). In each mutant, the transcript corresponding to the mutated gene was undetectable, indicating that the mutants isolated are true knock-out lines. The relative mRNA accumulation of the two remaining genes was not affected in any of the three mutants (Figure 2B). This result indicates that the disruption of an *ACO* gene does not alter the expression of the two other genes.

*ACO* genes encode aconitase, a key enzyme in the Krebs cycle located in the mitochondria. To determine whether these genes could encode cytosolic aconitase, both cytosolic and mitochondrial aconitase activities were measured from 10 days old plants grown in liquid medium. Mitochondrial matrix and cytosolic extracts were prepared, and the aconitase activity was measured in each extracts. The contamination of the cytosolic extract with mitochondrial proteins was determined by measuring the activity of the matrix-specific enzyme citrate synthase. In all experiments, the contamination of the cytosolic extracts by matrix mitochondria was estimated to be less than 5% (data not shown). In *aco1-1* mutant, the cytosolic and mitochondrial aconitase activities were reduced of about 75% and 20% respectively when compared to wild-type plants. In *aco3-1*, the reduction was around 25% for the cytosolic, and 55% for the mitochondrial activities. The cytosolic aconitase activity was not affected in the *aco2-1* background, whereas the mitochondrial activity was reduced of 20%. (Figure 2C). The mutations affected the ratio between mitochondrial and cytosolic activities. This indicates that, in our experimental conditions, ACO1 is mainly involved in the cytosolic activity, and ACO3 is responsible of the largest part of the mitochondrial activity.

### **Expression of *ACO* genes in *Arabidopsis***

The expression pattern of the three *ACO* genes *in planta* was investigated. Total RNA extracted from seeds, roots, leaves, stem, caulinary leaves and flowers was analyzed by northern hybridization using the *ACO* specific probes (Figure 3). The three genes present a very similar expression pattern, being expressed in all organs, except in the seed, where *ACO1* mRNA accumulation was undetectable, and *ACO2* and *ACO3* genes were weakly expressed. *ACO1* mRNA was more abundant in roots, stems and caulinary leaves. The highest level of expression of *ACO2* was detected in roots, caulinary leaves and flowers.

To gain further insight regarding the potential IRP activity of the proteins encoded by the *ACO* genes, we have first investigated the expression of the aconitase genes in standard, iron-excess and iron-starved conditions (Figure 4). Under iron-excess condition, the abundance of the *AtFer1* transcript increased rapidly. By contrast, the expression of the three aconitase genes was not affected by this treatment (Figure 4A). Under iron-deficient condition, the mRNA corresponding to the iron-starvation inducible gene *IRT1* [25, 32] accumulated two days after application of the treatment. Under such condition, the mRNA abundance of *ACO3* was not significantly affected comparatively to standard iron nutrition condition, whereas those corresponding to *ACO1* and *ACO2* were slightly decreased after three days of starvation (Figure 4B).

In animal cells, the switch between cytosolic aconitase and IRP activity is associated with a decrease of the cytosolic aconitase activity. To determine whether such a switch may occur in plants, we investigated whether iron addition or depletion may lead to a modulation of the cytosolic aconitase activity. Aconitase activity was measured on ten days old plants grown in liquid medium, in control conditions (standard medium), 3 hours after the addition of iron-citrate (final concentration 300  $\mu$ M), and after one day of growth in an iron-depleted medium. Cytosolic and mitochondrial aconitase activities were measured in wild-type and in the three *aco* mutants (Figure 4C). In wild-type plants, the iron treatment led to a small increase of the cytosolic aconitase activity of about 25%. The iron starvation did not significantly modulate the activity. In the three *aco* mutants, the effects of iron addition and depletion on the cytosolic aconitase activity were similar to those observed in wild-type plant. Both iron starvation and addition led to a slight decrease of mitochondrial aconitase activity in all the genetic backgrounds.

Taken together, our results indicate that the modulation of the plant iron status did not strongly affect the expression of *ACO* genes in *Arabidopsis*. Moreover, cytosolic aconitase activity was not greatly affected by iron addition or depletion. In the three loss-of-function mutants, the modulation of the cytosolic aconitase activity in response to the iron status was the same than in wild-type suggesting that neither *ACO1*, nor *ACO2*, nor *ACO3* activity is strongly affected by iron.

### Ferritin gene expression in *aco* mutants

The involvement of *Arabidopsis* aconitase in the regulation of iron-responsive genes expression was finally investigated by analyzing the expression of two ferritin genes in the different *aco* genetic backgrounds. The *AtFer1* and *AtFer3* genes were chosen since the corresponding mRNA and protein quickly accumulate in response to iron addition [12, 13, 33]. Moreover, in animal cells, ferritin genes are one of the primary targets of the IRE/IRP regulation. We first determined the kinetic of *AtFer1* and *AtFer3* mRNA accumulation in the wild type and in the three *aco* mutants in response to excess iron (Figure 5A). In none of the mutants the accumulation of the two ferritin mRNA was affected. The ferritin protein accumulation was also investigated in the three genetic backgrounds (Figure 5B). Total protein extracts were prepared before, 24 and 48 hours after iron addition. The same level of ferritin accumulated in the three mutants compared to the wild-type. These results show that ACO1, ACO2 and ACO3 are not involved in the regulation of plant ferritin expression in response to iron, neither at the transcriptional, nor at the post-transcriptional level.

### Functional redundancy between the cytosolic aconitase proteins

Our results indicated that ACO2 protein does not have cytosolic aconitase activity, at least in our experimental conditions (Figure 4C). On the other hand, in *aco1-1* and *aco3-1* mutants, the cytosolic aconitase activity is reduced of about 75% and 25% respectively in comparison to the wild-type (Figure 2 and 4C), indicating that the corresponding proteins represent the two major sources of plant cytosolic aconitase activity. The expression pattern of *ACO1* and *ACO3* genes are very similar (Figure 3), suggesting that the two proteins may, at least partially, be redundant. Thus, it can not be excluded that the absence of modulation of ferritin gene expression in the single *aco1-1* and *aco3-1* mutants (Figure 5) was due to a compensation mechanism between ACO1 and ACO3. In the way to isolate and characterize a double *aco1-aco3* mutant, the progenies of plants homozygous for one mutation and heterozygous for the other (namely *aco1aco1-ACO3aco3* and *ACO1aco1-aco3aco3*) were sowed, and the genotype of the progeny was analyzed by PCR to detect the wild-type and mutant alleles. More than 100 plants from the two progenies were analyzed, but we failed to identify a double *aco1aco1-aco3aco3* mutant, suggesting that a mutation in both *ACO1* and *ACO3* genes is lethal. Moreover, when examining the seeds in the siliques of *aco1aco1-ACO3aco3* and *ACO1aco1-aco3aco3* plants, some aborted seeds were systematically observed (Figure 6A). The proportion of aborted seeds in the progeny of the two parental lines was close to 25%, a value expected for a lethal double mutation (Figure 6B). Our results indicate that ACO1 and ACO3 protein activities are required for the development of the embryo, or for the proper

development of the seed, and as a consequence unable us to study ferritin expression in the double *aco1-aco3* mutant.

### **Identification of IRE and potential bacterial aconitase binding sites in the *Arabidopsis* genome**

Our results (Figure 5) show clearly that *Arabidopsis* ACO are not involved in the transcriptional activation of *AtFer1* and *AtFer3* ferritin genes. However, it must be pointed out that, most of the residues known to be essential for the RNA binding activity of rabbit IRP1 are conserved in *Arabidopsis* ACO proteins (Figure 1). Such an important aminoacid conservation is intriguing, and indicates that a nucleotide binding activity of these proteins has to be considered. These essential residues for the IRP activity are also conserved in the bacterial aconitase protein that has been shown to bind to motifs unrelated to IRE [18]. The exact recognized motif (or sequence) by bacterial aconitase is still unknown, but some conserved elements have been identified in the 3'-UTR of *acnA* and *acnB* genes [18]. The high conservation of residues among animal, plant and bacterial proteins suggests that plant aconitase may also have a RNA binding activity. This hypothesis is supported by the recent work of Moeder et al. [20] which shows that *Arabidopsis* ACO1 protein is able to bind to the 5'-UTR of *CSD2* superoxide dismutase transcript.

To further study the potential involvement of plant aconitase as a nucleotide binding protein, we took advantage of the availability of the whole *Arabidopsis* genome sequence to look for potential binding sites in the 5'- and 3'-UTR of all the transcripts. For this bioinformatic search, we used the animal IRE, and the sequences identified in *E. coli acnA* and *acnB* genes [18]. In animals, IREs are stem-loops made of 30 nucleotides with a bulge. The loop has a conserved sequence, 5' CAGUGN 3', N usually being a pyrimidine [34]. We performed a search with the loop consensus sequence surrounded by a stem consisting of at least 5 bases in 5' complementary to the 5 bases located in 3'. Using this rule, we found only 4 genes containing a putative IRE, one gene with the sequence in the 5'-UTR, and the three others in the 3'-UTR (Table 1). The binding site of the bacterial aconitase is still unknown, but from the sequence homologies between the 3'-UTRs of the two target genes *acnA* and *acnB*, Yang and Guest [18] have suggested that two paired motifs ACACAAUGC and CAUUUU may, at least partly, be involved in the formation of aconitase binding sites. We searched for these two paired motifs in the *Arabidopsis* genome, and found them in the 5'-UTR of two genes and in the 3'-UTR of 4 others (Table 1). Because the probability to find them in UTRs sequence is likely more than 99% due to chance, as indicated by the SMILE software [30], such sequences are unlikely to be functional.

## DISCUSSION

To directly address the question of a potential link between plant cytosolic aconitase and the regulation of ferritin expression, we took advantage of the availability of the *Arabidopsis thaliana* genome sequence. We searched for IRP1 and IRP2 homologues, and three proteins (ACO1 to -3) were identified. These IRP-like proteins were found to encode mitochondrial aconitase (Figures 2 and 4), a result consistent with studies which found the 3 ACO proteins in the mitochondrial proteome [35]. In animals, mitochondrial and cytosolic aconitases are encoded by distinct genes [36, 37]. It is not the case in *S. cerevisiae*, in which a unique gene encode both mitochondrial and cytosolic aconitase [38, 39]. In plants, several reports indicate that, like in yeast, both mitochondrial and cytosolic aconitase are encoded by the same genes, therefore suggesting a dual targeting of the proteins [40-42]. Therefore, the question we had to address was to determine whether or not the three identified aconitases were targeted to the cytosol. The contribution of each ACO protein to the cytosolic aconitase activity was estimated from the analysis of the *aco* knock-out mutants (Figure 2), and suggests that ACO1 and ACO3 are the two major proteins displaying a cytosolic aconitase activity. ACO2, which is present in the mitochondria [35, 43, 44] may be not targeted to the cytosol. Alternatively, our experimental conditions may not reveal the cytosolic aconitase activity of this protein. Our results bring additional information to the work of Moeder *et al* [20] who determine the total (cytosolic + mitochondria matrix) aconitase activity in various *aco* mutant genetic backgrounds. It has also to be mentioned that the *aco1-1* and *aco2-1* mutants we have characterized in this work are different alleles than those used by Moeder *et al* [20].

Our major goal was to determine whether or not cytosolic aconitase is involved in the regulation of ferritin expression in plants. To address this question, we first studied the effect of the plant iron status on *ACO* gene expression (Figure 4). At the mRNA level, neither iron excess, nor iron depletion modulated the expression of aconitase genes. Moreover, when measuring the effect of iron treatments on the cytosolic aconitase activity, no strong variations were observed in wild-type, as well as in the mutants (Figure 4). Consistent with an IRP1- cytosolic aconitase switch, a variation of the plant iron status should have led to a modulation of the cytosolic aconitase activity by affecting the Fe-S assembly of the protein. Finally, the direct evidence that *Arabidopsis* ACO are not involved in the regulation of ferritin expression was given by studying the expression of two ferritin genes at the mRNA and protein levels in the *aco* mutant genetic backgrounds. In the three *aco* mutants, both the level of *AtFer1* and *AtFer3* transcript accumulated and the amount of ferritin subunit were identical to those detected in the wild-type. A potential functional redundancy between ACO1 and ACO3 could explain the lack of effect of the mutations on ferritin expression. However,

we did not observe any compensation between the three aconitase genes (Figure 2A), since the mutation in one gene did not affect the expression of the two others. The remaining activity in *aco1-1* mutant (probably due to ACO3 activity) could be sufficient to explain the absence of modulation of ferritin expression. We therefore intend to isolate a double *aco1-1 aco3-1* mutant, but failed to, as the presence of the two mutations leads to the abortion of seeds. This result indicates that the cytosolic aconitase activity is essential for the proper formation of the embryo or for the development of the seed.

Beside the question of the involvement of cytosolic aconitase on the regulation of iron metabolism in plants, our work provides tools to study the impact of disturbing the glyoxylate and/or citric acid cycles on plant growth and metabolism. The relative contribution of each ACO isoform on the mitochondrial and cytosolic aconitase activities, on the metabolism [42], on the regulation of oxidative stress and on the establishment of defense against pathogens [20, 45] could be studied with the loss-of-function mutants.

As a complementary approach to determine whether the IRE/ IRP1-cytosolic aconitase switch may occur or not in plants, we performed a bioinformatic search for putative aconitase RNA binding sites in the 5'- and 3'-UTR of *Arabidopsis* transcripts. Only 10 genes contain one of these sequences (Table 1). Among them, 4 genes contained a putative IRE sequence, and the others 6 contained the two consensus sequences [18] found in the bacterial aconitase regulated genes. The low number of genes containing these elements raise therefore the question of their significance. Four genes encode unknown proteins, and among the others, none of them is obviously related to iron metabolism.

Recent results show that plant cytosolic aconitase protein may have a RNA binding activity. Indeed, *Arabidopsis* ACO1 is able to bind to the 5'-UTR of the *CDS2* superoxide dismutase transcript [20]. This result raises the interesting point that, like in animals, plant cytosolic aconitase may have a RNA binding activity. However, the *CDS2* aconitase binding site is not an IRE nor a bacterial aconitase binding site [20]. Our bioinformatic analysis, which indicates that animal and bacterial *cis*-acting sequences are probably not functional in plants, is consistent with this result, since the *CDS2* gene was not detected by our analysis. These data suggest that the potential RNA binding activity of plant aconitase proteins does not involve a canonical *cis*-acting sequence, but would be more likely related to the secondary structure of the RNA region. The identification of the nucleotides involved in the *CDS2* ACO1-binding site, and the search for other transcripts able to bind ACO1 will be of primary importance in the future. Even more important will be the demonstration that this *in vitro* binding activity does exist *in vivo*, and participates to the regulation of so far unknown biological functions.

## Acknowledgments

This work was funded by Institut National de la Recherche Agronomique and Centre National de la Recherche Scientifique, and by the Action Concertée Incitative “Biologie Cellulaire Moléculaire et Structurale” n° BCMS166 from the Ministère de l’Education Nationale, de l’Enseignement Supérieur et de la Recherche. NA and KR were supported by a thesis fellowship from the Ministère de l’Education Nationale, de l’Enseignement Supérieur et de la Recherche.

## REFERENCES

- 1 Guerinot, M. L. and Yi, Y. (1994) Iron: Nutritious, noxious, and not readily available. *Plant Physiol.* **104**, 815-820
- 2 Noctor, G. and Foyer, C. H. (1998) Ascorbate and glutathione: Keeping active oxygen under control. *Annu. Rev. Plant Physiol. Plant Mol. Biol.* **49**, 249-279
- 3 Harrison, P. M. and Arosio, P. (1996) The ferritins: Molecular properties, iron storage function and cellular regulation. *Biochim. Biophys. Acta* **1275**, 161-203
- 4 Hentze, M. W. and Kuhn, L. C. (1996) Molecular control of vertebrate iron metabolism: mRNA-based regulatory circuits operated by iron, nitric oxide, and oxidative stress. *Proc. Natl. Acad. Sci. U. S. A.* **93**, 8175-8182
- 5 Klausner, R. D., Rouault, T. A. and Harford, J. B. (1993) Regulating the fate of mRNA: The control of cellular iron metabolism. *Cell* **72**, 19-28
- 6 Hirling, H., Henderson, B. R. and Kuhn, L. C. (1994) Mutational analysis of the [4Fe-4S]-cluster converting iron regulatory factor from its RNA-binding form to cytoplasmic aconitase. *EMBO J.* **13**, 453-461
- 7 Gardner, P. R., Raineri, I., Epstein, L. B. and White, C. W. (1995) Superoxide radical and iron modulate aconitase activity in mammalian cells. *J. Biol. Chem.* **270**, 13399-13405
- 8 Rouault, T. A. (2006) The role of iron regulatory proteins in mammalian iron homeostasis and disease. *Nat. Chem. Biol.* **2**, 406-414
- 9 Peyret, P., Perez, P. and Alric, M. (1995) Structure, genomic organization, and expression of the *Arabidopsis thaliana* aconitase gene. Plant aconitase show significant homology with mammalian iron-responsive element-binding protein. *J. Biol. Chem.* **270**, 8131-8137
- 10 Navarre, D. A., Wendehenne, D., Durner, J., Noad, R. and Klessig, D. F. (2000) Nitric oxide modulates the activity of tobacco aconitase. *Plant Physiol.* **122**, 573-582
- 11 Murgia, I., Delledonne, M. and Soave, C. (2002) Nitric oxide mediates iron-induced ferritin accumulation in *Arabidopsis*. *Plant J.* **30**, 521-528
- 12 Petit, J. M., Briat, J. F. and Lobréaux, S. (2001) Structure and differential expression of the four members of the *Arabidopsis thaliana* ferritin gene family. *Biochem. J.* **359**, 575-582
- 13 Arnaud, N., Murgia, I., Boucherez, J., Briat, J. F., Cellier, F. and Gaymard, F. (2006) An iron-induced nitric oxide burst precedes ubiquitin-dependent protein degradation for *Arabidopsis AtFer1* ferritin gene expression. *J. Biol. Chem.* **281**, 23579-23588
- 14 Verniquet, F., Gaillard, J., Neuburger, M. and Douce, R. (1991) Rapid inactivation of plant aconitase by hydrogen peroxide. *Biochem. J.* **276**, 643-648

- 15 Lescure, A. M., Proudhon, D., Pesey, H., Ragland, M., Theil, E. C. and Briat, J. F. (1991) Ferritin gene transcription is regulated by iron in soybean cell cultures. *Proc. Natl. Acad. Sci. U. S. A.* **88**, 8222-8226
- 16 Rothenberger, S., Mullner, E. W. and Kuhn, L. C. (1990) The mRNA-binding protein which controls ferritin and transferrin receptor expression is conserved during evolution. *Nucleic Acids Res.* **18**, 1175-1179
- 17 Brown, P. H., Daniels-McQueen, S., Walden, W. E., Patino, M. M., Gaffield, L., Bielser, D. and Thach, R. E. (1989) Requirements for the translational repression of ferritin transcripts in wheat germ extracts by a 90-kda protein from rabbit liver. *J. Biol. Chem.* **264**, 13383-13386
- 18 Tang, Y. and Guest, J. R. (1999) Direct evidence for mRNA binding and post-transcriptional regulation by *Escherichia coli* aconitases. *Microbiology* **145**, 3069-3079
- 19 Tang, Y., Quail, M. A., Artymiuk, P. J., Guest, J. R. and Green, J. (2002) *Escherichia coli* aconitases and oxidative stress: Post-transcriptional regulation of *sodA* expression. *Microbiology* **148**, 1027-1037
- 20 Moeder, W., Del Pozo, O., Navarre, D. A., Martin, G. B. and Klessig, D. F. (2006) Aconitase plays a role in regulating resistance to oxidative stress and cell death in *Arabidopsis* and *Nicotiana benthamiana*. *Plant Mol. Biol.* **63**, 273-287
- 21 Alonso, J. M., Stepanova, A. N., Leisse, T. J., Kim, C. J., Chen, H., Shinn, P., Stevenson, D. K., Zimmerman, J., Barajas, P., Cheuk, R., Gadrinab, C., Heller, C., Jeske, A., Koesema, E., Meyers, C. C., Parker, H., Prednis, L., Ansari, Y., Choy, N., Deen, H., Geralt, M., Hazari, N., Hom, E., Karnes, M., Mulholland, C., Ndubaku, R., Schmidt, I., Guzman, P., Aguilar-Henonin, L., Schmid, M., Weigel, D., Carter, D. E., Marchand, T., Risseuw, E., Brogden, D., Zeko, A., Crosby, W. L., Berry, C. C. and Ecker, J. R. (2003) Genome-wide insertional mutagenesis of *Arabidopsis thaliana*. *Science* **301**, 653-657
- 22 Rosso, M. G., Li, Y., Strizhov, N., Reiss, B., Dekker, K. and Weisshaar, B. (2003) An *Arabidopsis thaliana* T-DNA mutagenized population (gabi-kat) for flanking sequence tag-based reverse genetics. *Plant Mol. Biol.* **53**, 247-259
- 23 Cellier, F., Conejero, G., Ricaud, L., Luu, D. T., Lepetit, M., Gosti, F. and Casse, F. (2004) Characterization of AtCHX17, a member of the cation/H<sup>+</sup> exchangers, CHX family, from *Arabidopsis thaliana* suggests a role in K<sup>+</sup> homeostasis. *Plant J.* **39**, 834-846
- 24 Lobréaux, S., Hardy, T. and Briat, J. F. (1993) Abscisic acid is involved in the iron-induced synthesis of maize ferritin. *EMBO J.* **12**, 651-657
- 25 Vert, G., Grotz, N., Dedaldechamp, F., Gaymard, F., Guerinot, M. L., Briat, J. F. and Curie, C. (2002) IRT1, an *Arabidopsis* transporter essential for iron uptake from the soil and for plant growth. *Plant Cell* **14**, 1223-1233
- 26 Schaffner, W. and Weissmann, C. (1973) A rapid, sensitive, and specific method for the determination of protein in dilute solution. *Anal. Biochem.* **56**, 502-514
- 27 Lobréaux, S., Massenet, O. and Briat, J. F. (1992) Iron induces ferritin synthesis in maize plantlets. *Plant Mol. Biol.* **19**, 563-575
- 28 Laemmli, U. K. (1970) Cleavage of structural proteins during the assembly of the head of bacteriophage T4. *Nature* **227**, 680-685
- 29 Dellagi, A., Rigault, M., Segond, D., Roux, C., Kraepiel, Y., Cellier, F., Briat, J. F., Gaymard, F. and Expert, D. (2005) Siderophore-mediated upregulation of *Arabidopsis* ferritin expression in response to *Erwinia chrysanthemi* infection. *Plant J.* **43**, 262-272

- 30 Marsan, L. and Sagot, M. F. (2000) Algorithms for extracting structured motifs using a suffix tree with an application to promoter and regulatory site consensus identification. *J. Comput. Biol.* **7**, 345-362
- 31 Walden, W. E., Selezneva, A. I., Dupuy, J., Volbeda, A., Fontecilla-Camps, J. C., Theil, E. C. and Volz, K. (2006) Structure of dual function Iron Regulatory Protein 1 complexed with ferritin IRE-RNA. *Science* **314**, 1903-1908
- 32 Eide, D., Broderius, M., Fett, J. and Guerinot, M. L. (1996) A novel iron-regulated metal transporter from plants identified by functional expression in yeast. *Proc. Natl. Acad. Sci. U. S. A.* **93**, 5624-5628
- 33 Gaymard, F., Boucherez, J. and Briat, J. F. (1996) Characterization of a ferritin mRNA from *Arabidopsis thaliana* accumulated in response to iron through an oxidative pathway independent of abscisic acid. *Biochem. J.* **318**, 67-73
- 34 Theil, E. C. (1994) Iron regulatory elements (IREs): A family of mRNA non-coding sequences. *Biochem. J.* **304**, 1-11
- 35 Heazlewood, J. L., Tonti-Filippini, J. S., Gout, A. M., Day, D. A., Whelan, J. and Millar, A. H. (2004) Experimental analysis of the *Arabidopsis* mitochondrial proteome highlights signaling and regulatory components, provides assessment of targeting prediction programs, and indicates plant-specific mitochondrial proteins. *Plant Cell* **16**, 241-256
- 36 Eanes, R. Z. and Kun, E. (1971) Separation and characterization of aconitate hydratase isoenzymes from pig tissues. *Biochim. Biophys. Acta* **227**, 204-210
- 37 Kennedy, M. C., Mende-Mueller, L., Blondin, G. A. and Beinert, H. (1992) Purification and characterization of cytosolic aconitase from beef liver and its relationship to the iron-responsive element binding protein. *Proc. Natl. Acad. Sci. U. S. A.* **89**, 11730-11734
- 38 Gangloff, S. P., Marguet, D. and Lauquin, G. J. (1990) Molecular cloning of the yeast mitochondrial aconitase gene (*aco1*) and evidence of a synergistic regulation of expression by glucose plus glutamate. *Mol. Cell. Biol.* **10**, 3551-3561
- 39 Regev-Rudzki, N., Karniely, S., Ben-Haim, N. N. and Pines, O. (2005) Yeast aconitase in two locations and two metabolic pathways: seeing small amounts is believing. *Mol. Biol. Cell* **16**, 4163-4171
- 40 Brouquisse, R., Nishimura, M., Gaillard, J. and Douce, R. (1987) Characterization of a cytosolic aconitase in higher plant cells. *Plant Physiol.* **84**, 1402-1407
- 41 De Bellis, L., Tsugeki, R., Alpi, A. and Nishimura, M. (1993) Purification and characterization of aconitase isoforms from etiolated pumpkin cotyledons. *Physiol. Plant.* **88**, 485-492
- 42 Carrari, F., Nunes-Nesi, A., Gibon, Y., Lytovchenko, A., Loureiro, M. E. and Fernie, A. R. (2003) Reduced expression of aconitase results in an enhanced rate of photosynthesis and marked shifts in carbon partitioning in illuminated leaves of wild species tomato. *Plant Physiol.* **133**, 1322-1335
- 43 Kruft, V., Eubel, H., Jansch, L., Werhahn, W. and Braun, H. P. (2001) Proteomic approach to identify novel mitochondrial proteins in *Arabidopsis*. *Plant Physiol.* **127**, 1694-1710
- 44 Millar, A. H., Sweetlove, L. J., Giege, P. and Leaver, C. J. (2001) Analysis of the *Arabidopsis* mitochondrial proteome. *Plant Physiol.* **127**, 1711-1727
- 45 Cots, J. and Widmer, F. (1999) Germination, senescence and pathogenic attack in soybean (*glycine max.* L.): identification of the cytosolic aconitase participating in the glyoxylate cycle. *Plant Sci.* **149**, 95-104

## LEGENDS TO FIGURES

Figure 1. Sequence alignment of the deduced *Arabidopsis* aconitases with human IRP1 and IRP2. The human IRP1 (Genbank accession NP002188) and IRP2 (Genbank accession NP004127) was aligned with their *Arabidopsis* homologues At4g35830 (ACO1), At4g26970 (ACO2) and At2g05710 (ACO3). Identical and similar residues between at least three proteins are boxed in black and grey respectively. Gaps were introduced to maximize alignment. Aminoacids are numbered from the translational start methionine. Stars indicate aminoacids directly interacting with the RNA loop of the IRE [31]. The three cysteine residues involved in the 4Fe-4S cluster formation in IRP1 are indicated by squares.

Figure 2. Isolation of *aco* knock-out mutants. A. Characterization of the *aco1-1*, *aco2-1* and *aco3-1* mutant lines. The diagram illustrates the site of insertion on the T-DNA in the different genes. Boxes and lines represent exons and introns, respectively. The gene/ T-DNA junction sequences are indicated. The gene sequences are indicated in bold type, the T-DNA sequences are in upper case, and additional sequences found at the junctions are in lower case. LB: left border of the T-DNA. Numbering is given relative to the first codon of the translation initiation site. B. Expression of *ACO* genes in wild-type and *aco* mutants. Wild-type *Arabidopsis* (Col), *aco1-1*, *aco2-1* and *aco3-1* plantlets were grown for 10 days in liquid medium. RNA was analyzed by northern blotting and hybridized successively with the *ACO1*, *ACO2*, *ACO3* and *25S* probes. *25S* RNA abundance was shown as loading control. C. Effect of the mutations on cytosolic and mitochondrial aconitase activities. Plants were grown as described in B. Cytosolic and matrix extracts were prepared, and the aconitase activities were measured. Results are presented as the percentage of the cytosolic (black histograms) and mitochondrial (white histograms) aconitase activities measured for Col plants. Bars correspond to the standard deviation from three independent experiments.

Figure 3. Expression of aconitase genes in the different organs of *Arabidopsis*. Plants were grown in hydroponic conditions for 5 weeks. Total RNA was extracted from seeds (S), roots (R), rosette leaves (L), stem (St), caulinary leaves (CL) and flowers (F), and analyzed by northern blot as described in the legend to figure 2.

Figure 4. Effect of iron nutrition on aconitase gene expression and aconitase activities. A. Effect of excess iron on *ACO* mRNA accumulation. Wild-type plantlets (Col) were grown as described in the legend to figure 2. Iron-citrate (final concentration 300  $\mu$ M) was added, and plantlets were collected

before (0), and 1, 3 and 6 h after iron addition. Northern blot was performed as described in the legend to figure 2. The mRNA abundance of *AtFer1* was used as a positive control of the iron treatment. B. Effect of iron depletion on *ACO* mRNA accumulation. Col plantlets were grown for 7 days as described in the legend to figure 2, and transferred in a medium without iron. Plantlets were collected before (0), and 24, 48 and 72 hours after the transfer. Northern blot was performed as described in the legend to figure 2. The mRNA abundance of *IRT1* was used as a positive control of the treatment. C. Effect of iron status on aconitase activities. Col, *aco1-1*, *aco2-1* and *aco3-1* plantlets were grown for 10 days in liquid medium (C), 300  $\mu$ M Fe-citrate was added for 3 h (+Fe), or plantlets were grown for an additional day in iron-free medium (-Fe). Cytosolic and matrix extracts were prepared, and the cytosolic (black histograms) and mitochondrial (white histograms) aconitase activities were measured. Bars correspond to the standard deviation from three independent experiments.

Figure 5. Effect of *aco* mutations on ferritin expression. A. *AtFer1* and *AtFer3* mRNA abundance in *aco* mutants. Col, *aco1-1*, *aco2-1* and *aco3-1* plantlets were grown for 10 days in liquid medium. Iron-citrate was added (300  $\mu$ M final), and plantlets were collected before (0), 1, 3 and 6 h after the treatment. RNA was extracted, analyzed by northern blotting, and hybridized successively with the *AtFer1*, *AtFer3*, *EF1 $\alpha$*  and *25S* probes. *EF1 $\alpha$*  mRNA and *25S* RNA abundance were used as loading controls. B. Effect of the mutation on ferritin protein accumulation in response to iron. Col, *aco1-1*, *aco2-1* and *aco3-1* plantlets were grown for 10 days in liquid medium. Iron-citrate was added (300  $\mu$ M final), and plantlets were collected before (0), 24 and 48 h after the treatment. Total protein were extracted. Ten  $\mu$ g protein extracts were loaded for each lane. A polyclonal serum (1/20000 dilution) raised against *AtFer1* protein was used for immunodetection. A coomassie blue stained gel is shown as loading control.

Figure 6. The double mutant *aco1-1 aco3-1* is lethal. A. Aborted seeds present in siliques of a plant mutant in *ACO1* gene and heterozygous at the *ACO3* locus. Wild type (Col) and mutant (genotype *aco1-1 aco1-1 ACO3 aco3-1*) plants were grown in green house and siliques were collected just before dehiscence. Siliques were opened and seeds were examined under binocular. All the seeds were normal in Col plants (left), whereas some were aborted in the mutant (right, aborted seeds are indicated by arrows). B. Proportion of aborted seeds in the progeny of plants mutant at one locus, and heterozygous at the second. Wild-type (Col) and mutant plants (genotype *aco1-1 aco1-1 ACO3 aco3-1* and *ACO1 aco1-1 aco3-1 aco3-1*) were grown in green house, and seeds were collected. The proportion of aborted seeds was estimated visually under binocular.

Table 1. Putative IRE and bacterial aconitase binding sites in the UTR of *Arabidopsis thaliana* genes.

<i>cis</i> element	location	sequence	AGI	function
IRE	3'-UTR	<b>CUGGAUCAGUGGAUCUA</b>	At1g63490	jumonji domain-containing protein
	3'-UTR	<b>CAUAAUCAGUGUAUUUAU</b>	At3g02520	14-3-3 protein
	5'-UTR	<b>CAAAAUCAGUGAAUUUU</b>	At3g54130	josephin protein family
	3'-UTR	<b>CUUGUGCAGUGGCACAA</b>	At3g61380	unknown
<hr/>				
acn binding domain	5'-UTR	ACACAAUGC and CAUUUU	At1g35510	unknown
	5'-UTR	ACACAAUGC and CAUUUU	At2g40460	proton-dependent oligopeptide transporter
	3'-UTR	ACACAAUGC and CAUUUU	At3g10220	tubulin folding cofactor B
	3'-UTR	ACACAAUGC and CAUUUU	At5g01450	unknown
	3'-UTR	ACACAAUGC and CAUUUU	At5g28150	unknown
	3'-UTR	ACACAAUGC and CAUUUU	At5g63780	zinc finger

For each accession, the location (in the 5'- or 3'-UTR) of the putative element in the transcript is indicated. For IRE sequence, the corresponding sequence found in the database is given. The bases of the IRE consensus are indicated in bold type. The AGI number, and function of the corresponding genes are indicated.

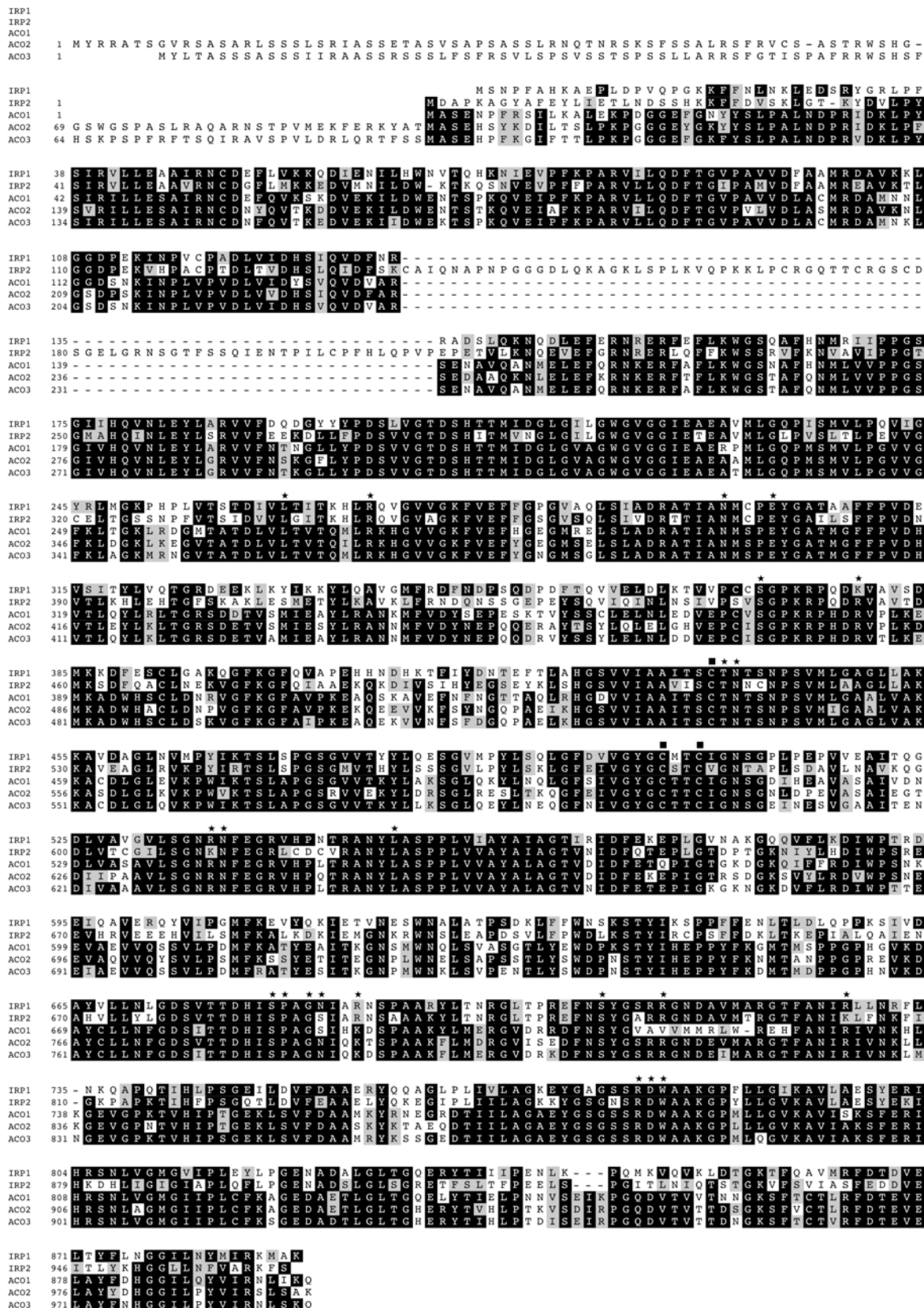


Figure 1

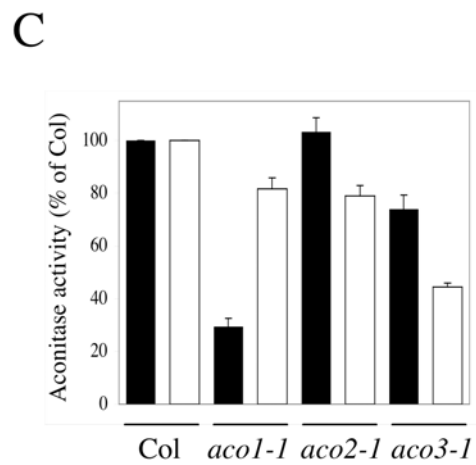
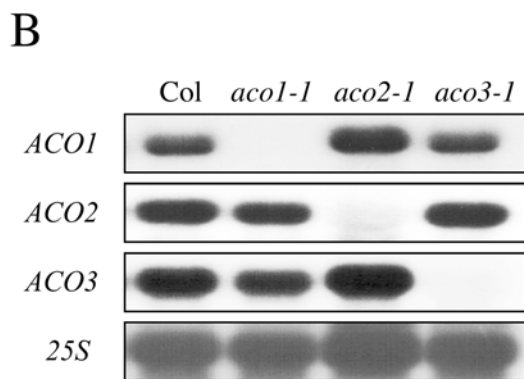
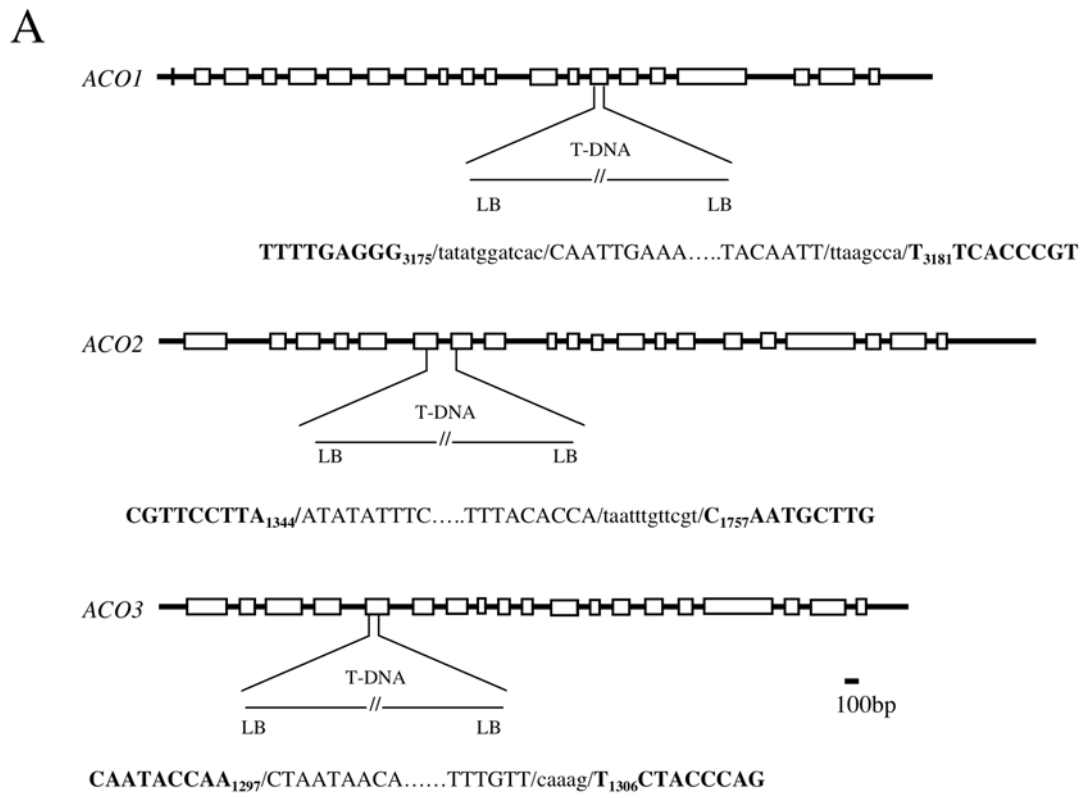


Figure 2

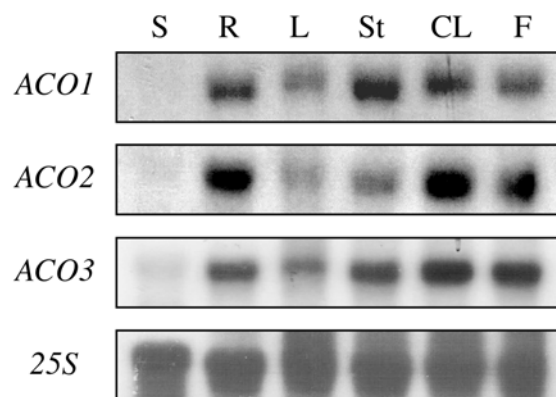


Figure 3

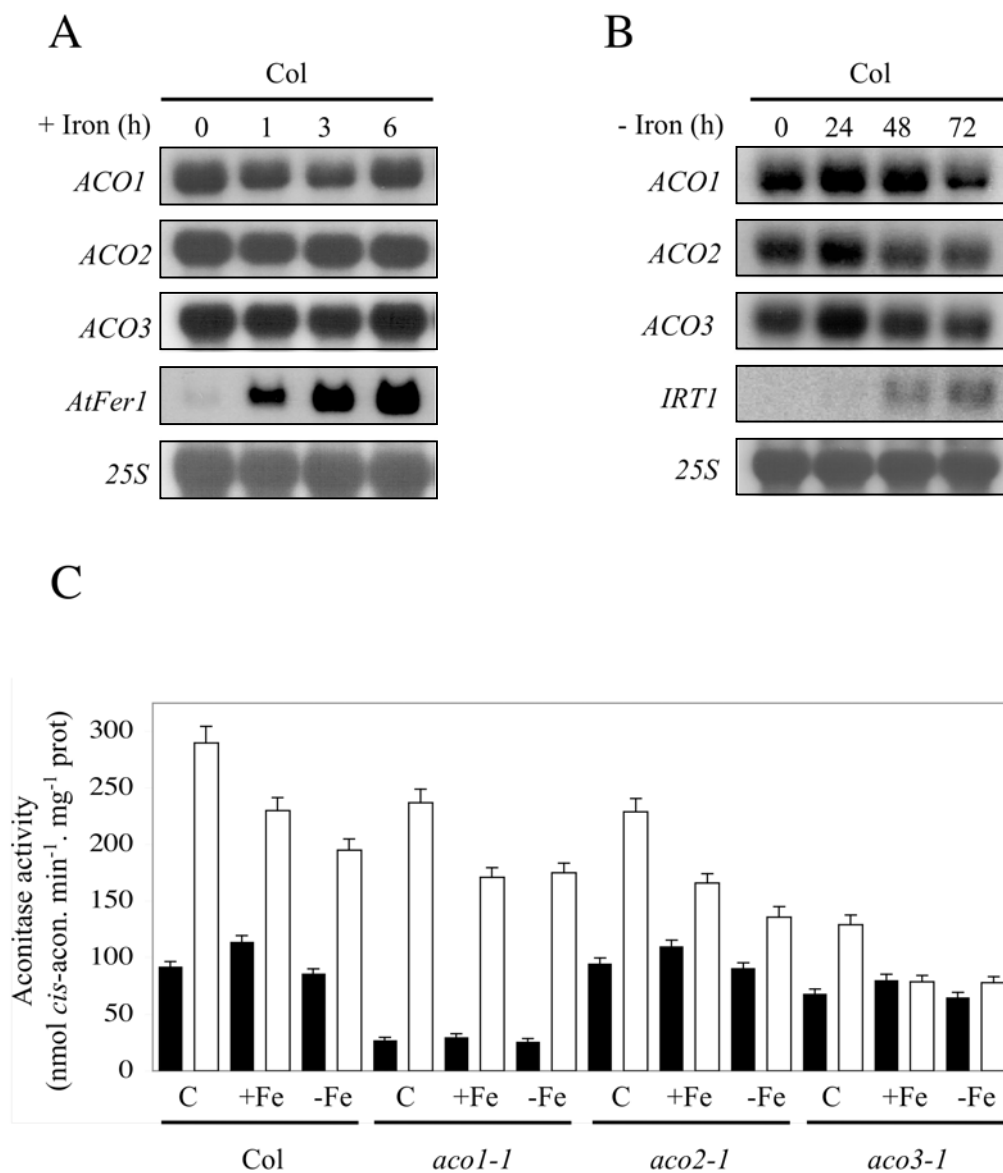


Figure 4

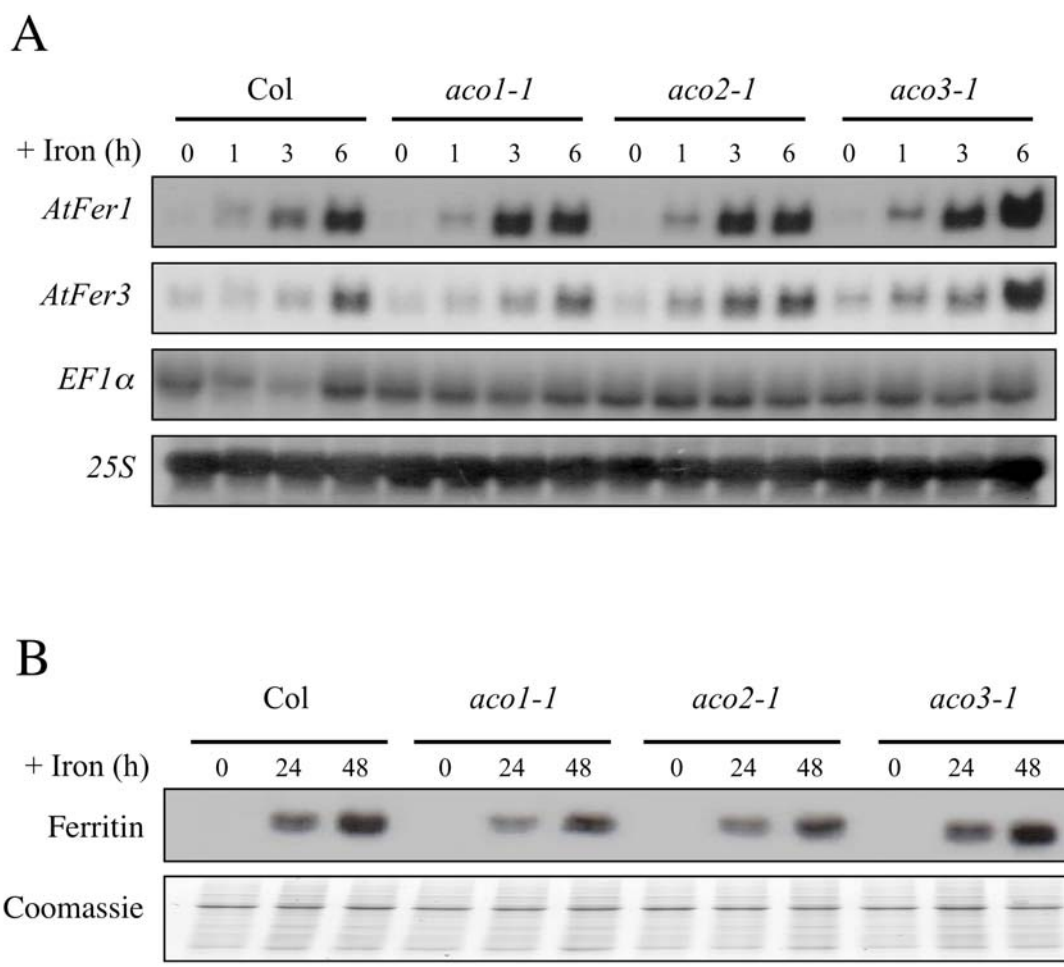
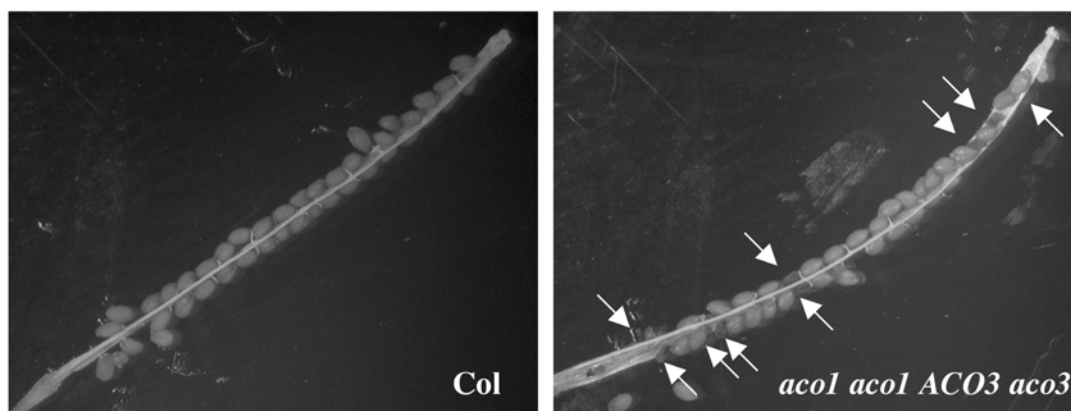


Figure 5

A



B

Genotype	Total seeds	Aborted seeds	Proportion aborted (%)
Col	136	1	0.73
<i>ACO1 aco1-1 aco3-1 aco3-1</i>	171	41	23.97
<i>aco1-1 aco1-1 ACO3 aco3-1</i>	328	85	25.91

Figure 6